KU LEUVEN

Citation	Frederik Debrouwere, Wannes Van Loock, Goele Pipeleers, Moritz Diehl, Jan Swevers, Joris De Schutter **Convex Time-Optimal Robot Path Following with Cartesian Acceleration and Inertial Force and Torque Constraints** Proceedings of the Institution of Mechanical Engineers I, Journal of Systems and Control Engineering, 227 (10), 724-732
Archived version	Author manuscript: the content is identical to the content of the published paper, but without the final typesetting by the publisher
Published version	insert link to the published version of your paper http://pii.sagepub.com/content/227/10/724.abstract
Journal homepage	insert link to the journal homepage of your paper http://pii.sagepub.com/
Author contact	your email Frederik.Debrouwere@kuleuven.be your phone number *+ 32 (0)16 322539*
IR	url in Lirias https://lirias.kuleuven.be/handle/123456789/412352

(article begins on next page)

Convex Time-Optimal Robot Path Following with Cartesian Acceleration and Inertial Force and Torque Constraints

Frederik Debrouwere*, Wannes Van Loock*, Goele Pipeleers*, Moritz Diehl†, Jan Swevers* and Joris De Schutter*
*Department of Mechanical Engineering, Division PMA, KU Leuven, BE-3001 Heverlee, Belgium
Email: Frederik.Debrouwere@mech.kuleuven.be
†Department of Electrical Engineering, Division SCD, KU Leuven, BE-3001 Heverlee, Belgium

***Abstract*—In time-optimal robot path following a predetermined geometric trajectory is followed exactly in a time-optimal way considering system constraints, e.g. actuator constraints. For a simplified robotic manipulator, this optimization problem can be reformulated into a convex optimization problem when only considering some system constraints. In this paper the convex approach is extended to account for Cartesian acceleration constraints, and in turn account for inertial forces an torques acting on a load held by the robot. The focus of this paper lies on the reformulation of these Cartesian acceleration and inertial forces and torques to preserve the convexity of the optimization problem. We present a series of applications that result in solving a convex optimization problem, illustrating the practicality of the proposed reformulations.**

I. Introduction

Path following deals with the problem of following a geometric path without any preassigned timing information. Many industrial robot tasks, such as welding, glueing, laser cutting and milling can be cast as path following problems. In addition, path following is often considered to be the low level stage in a decoupled motion planning approach [1], [2]. First, a high level planner determines a geometric path ignoring the system dynamics but taking into account geometric path constraints. Second, an optimal trajectory along the geometric path is determined that accounts for the system dynamics and limitations. Since the dynamics along a geometric path can be described by a scalar path coordinate s and its time derivatives [1], [2], the decoupled approach simplifies the motion planning problem to a great extent. Recently it was shown that the path following problem for a robotic manipulator with simplified constraints can be cast as a *convex* optimization problem [3]. This guarantees the efficient computation of globally optimal solutions.

This paper extends the framework developed in [3] such that it can deal with Cartesian acceleration constraints and constraints on inertial forces and torques acting on a load, attached to the robot, while preserving convexity. This work is based on the ideas presented in [4]. The theoretical part on the Cartesian and inertial force and torque constraints has been extended to be general. Furthermore, some applications have been added to illustrate the practicality of the proposed reformulations. In the original paper [4], optimal tool selection was considered by including inertial load effects into the robot dynamics. This is an application of the inertial force and torque reformulation. Since this is considered there it is not included in this paper.

In many applications it is useful to include a Cartesian acceleration constraint on the motion of the end effector of a robotic manipulator, e.g. in moving fragile objects [5]. In this case, the Cartesian acceleration of the robot end effector, expressed in the end effector frame must be constrained to avoid the objects from being damaged. We show that these types of constraints preserve the convexity of the optimization problem.

Furthermore, in other applications it is useful to include constraints on the inertial forces and torques, acting on a load held by the robot. Examples are found in moving loosely stacked objects on a pallet (also referred to as the tip slip lift problem) to prevent the objects from falling off, or moving an open barrel filled with a liquid to prevent overflowing of the liquid. We show that these force and torque constraints are related to Cartesian acceleration constraints and that they preserve convexity.

Similar time-optimal trajectory generation problems have challenged scientists for a long time. However, they came to applicable solutions only with the disposability of computers, mainly starting in the 1980s. This allows for efficient numerical computations of the optimal solution. A more detailed review is given in [1].

The paper is organized as follows. Section II reviews the convex reformulation of the time-optimal path following problem of [3]. Section III presents the proposed additions to the convex framework. Here the derivation of the Cartesian acceleration and inertial force and torque formulations are treated in detail. Section IV illustrates the practical use of the proposed extensions with some applications, simulations and experiments.

Throughout the paper we indicate scalars with a lower-case letter, e.g. n, vectors with a bold lower-case letter, e.g. $\boldsymbol{q}$ and matrices with an upper-case letter, e.g. M. Furthermore, ${}^{v}_{f}\boldsymbol{v}^{o}_{w}$ indicates the velocity of the reference point v on the body with frame $\{o\}$ with respect to the frame $\{w\}$, expressed in the frame $\{f\}$, and ${}_{f}\boldsymbol{f}^{o[u]}$ indicates the force on the body with

frame $\{o\}$, attached to the frame $\{u\}$, expressed in the frame $\{f\}$.

II. Problem statement

Consider a robotic manipulator with n degrees of freedom and joint angles $\boldsymbol{q} \in \mathbb{R}^n$. The equations of motion are given by

$$\boldsymbol{\tau} = M(\boldsymbol{q})\ddot{\boldsymbol{q}} + C(\boldsymbol{q}, \dot{\boldsymbol{q}})\dot{\boldsymbol{q}} + \boldsymbol{g}(\boldsymbol{q}), \tag{1}$$

where $\boldsymbol{\tau} \in \mathbb{R}^n$ are the joint torques, $M \in \mathbb{R}^{n\times n}$ is the mass matrix, $C \in \mathbb{R}^{n\times n}$ is a matrix, linear in $\dot{\boldsymbol{q}}$, accounting for Coriolis and centrifugal effects and, $\boldsymbol{g}$ is a vector accounting for gravity and other position dependent torques.

Consider a prescribed geometric path $\boldsymbol{q}(s)$ as a function of a scalar path coordinate s, given in joint space coordinates. The time dependence of the path is determined through $s(t)$. Without loss of generality it is assumed that the trajectory starts at $t = 0$, ends at $t = T$ and, $0 = s(0) \leq s(t) \leq s(T) = 1$. It is furthermore assumed that we always move forward along the path, i.e. $\dot{s}(t) \geq 0, \forall t \in [0, T]$.

Using the chain-rule we rewrite joint velocities and accelerations as

$$\dot{\boldsymbol{q}}(s) = \boldsymbol{q}'(s)\dot{s} \text{ and, } \ddot{\boldsymbol{q}}(s) = \boldsymbol{q}''(s)\dot{s}^2 + \boldsymbol{q}'(s)\ddot{s}, \tag{2}$$

where $\boldsymbol{q}' = d\boldsymbol{q}(s)/ds$ and, $\boldsymbol{q}'' = d^2\boldsymbol{q}(s)/ds^2$. Substitution of the above equations in (1) projects the equations of motion onto the path [3]:

$$\boldsymbol{\tau}(s) = \boldsymbol{m}(s)\ddot{s} + \boldsymbol{c}(s)\dot{s}^2 + \boldsymbol{g}(s). \tag{3}$$

By introducing the variables

$$b(s) = \dot{s}^2 \text{ and } a(s) = \ddot{s}, \tag{4}$$

it was shown in [3] that the time-optimal path following problem is transformed into a *convex* optimization problem. Indeed, since $b(s) \geq 0$, the total motion time

$$T = \int_0^T 1dt = \int_0^1 \frac{1}{\dot{s}} ds = \int_0^1 \frac{1}{\sqrt{b(s)}} ds,$$

is a convex function. Furthermore torque constraints are linear in $b(s)$ and $a(s)$. The convex time-optimal path following problem is then reformulated as

$$\begin{aligned}
\underset{a(.),b(.)}{\text{minimize}} \quad & \int_0^1 \frac{1}{\sqrt{b(s)}} ds, \\
\text{subject to} \quad & \boldsymbol{\tau}(s) = \boldsymbol{m}(s)a(s) + \boldsymbol{c}(s)b(s) + \boldsymbol{g}(s), \\
& \underline{\boldsymbol{\tau}}(s) \leq \boldsymbol{\tau}(s) \leq \overline{\boldsymbol{\tau}}(s), \\
& b(0) = \dot{s}_0^2, b(1) = \dot{s}_T^2, \\
& b(s) \geq 0, \\
& b'(s) = 2a(s), \\
& \text{for } s \in [0, 1].
\end{aligned} \tag{5}$$

Where $\underline{\boldsymbol{\tau}}(s) \leq \boldsymbol{\tau}(s) \leq \overline{\boldsymbol{\tau}}(s)$ ensures that the actuator limits are not exceeded.

In [3] some additions are listed that preserve the convexity of the optimization problem, e.g. joint velocity and acceleration constraints and Cartesian velocity constraints. Cartesian acceleration constraints were already mentioned in [3] but not treated in detail.

III. Additions to the framework

This section discusses the addition of constraints on Cartesian accelerations and inertial forces and torques to the convex framework stated above.

A. Cartesian acceleration

In this section, it is shown that the Cartesian acceleration of any frame of the robot (link, end effector, ...) with respect to any other frame (link, end effector, base, ...) linearly depends on the optimization variables $a(s)$ and $b(s)$. A special case which has a lot of practical use is the acceleration of the end effector frame $\{ee\}$ with respect to the robot base frame $\{bs\}$.

The Cartesian acceleration is derived from the expression of the velocity twist, ${}^v_f\boldsymbol{t}^o_w \in \mathbb{R}^{6\times 1}$, representing the Cartesian translational ${}^v_f\boldsymbol{v}^o_w \in \mathbb{R}^{3\times 1}$ and rotational ${}^v_f\boldsymbol{\omega}^o_w \in \mathbb{R}^{3\times 1}$ velocity of the reference point v on the body with frame $\{o\}$ with respect to the frame $\{w\}$, expressed in the frame $\{f\}$.

$${}^v_f\boldsymbol{t}^o_w(s) = \begin{pmatrix} {}^v_f\boldsymbol{v}^o_w(s) \\ {}^v_f\boldsymbol{\omega}^o_w(s) \end{pmatrix}.$$

The Cartesian velocity twist and joint velocity are related by the geometric Jacobian ${}^v_f J^o_w(\boldsymbol{q}) \in \mathbb{R}^{6\times n}$ [6]:

$${}^v_f\boldsymbol{t}^o_w(s) = {}^v_f J^o_w(\boldsymbol{q}(s))\, \dot{\boldsymbol{q}}(s). \tag{6}$$

Now, the Cartesian acceleration twist (time derivative of the velocity twist) is calculated by differentiating (6) to time

$${}^v_f\dot{\boldsymbol{t}}^o_w(s) = \begin{pmatrix} {}^v_f\dot{\boldsymbol{v}}^o_w(s) \\ {}^v_f\dot{\boldsymbol{\omega}}^o_w(s) \end{pmatrix} = {}^v_f J^o_w(s)\, \ddot{\boldsymbol{q}}(s) + {}^v_f \dot{J}^o_w(s)\, \dot{\boldsymbol{q}}(s). \tag{7}$$

In order to derive the relation between the Cartesian acceleration and the optimization variables, the time derivative of the Jacobian is reformulated

$${}^v_f \dot{J}^o_w(s) = \frac{\partial \left({}^v_f J^o_w(s) \right)}{\partial s} \frac{ds}{dt} = {}^v_f J^{o\prime}_w(s)\dot{s}, \tag{8}$$

Substituting (2), (4) and (8) into (7) results in the Cartesian acceleration twist

$${}^v_f\dot{\boldsymbol{t}}^o_w(s) = {}^v_f\boldsymbol{j}_{\boldsymbol{a}}{}^o_w(s)a(s) + {}^v_f\boldsymbol{j}_{\boldsymbol{b}}{}^o_w(s)b(s), \tag{9}$$

with

$$\begin{aligned}
{}^v_f\boldsymbol{j}_{\boldsymbol{a}}{}^o_w(s) &= {}^v_f J^o_w(s)\boldsymbol{q}'(s), \\
{}^v_f\boldsymbol{j}_{\boldsymbol{b}}{}^o_w(s) &= {}^v_f J^o_w(s)\boldsymbol{q}''(s) + {}^v_f J^{o\prime}_w(s)\boldsymbol{q}'(s),
\end{aligned}$$

which is linear in $a(s)$ and $b(s)$. Hence adding an inequality constraint on the Cartesian acceleration twist to optimization problem (5) preserves convexity. This derivation is independent of the choice of v, $\{f\}$, $\{o\}$ and $\{w\}$, which can be any frame on the robot. A special case is the acceleration of the end effector with respect to the base frame of the robot, hence $\{o\} = \{ee\}$ and $\{w\} = \{bs\}$. For this choice there are three

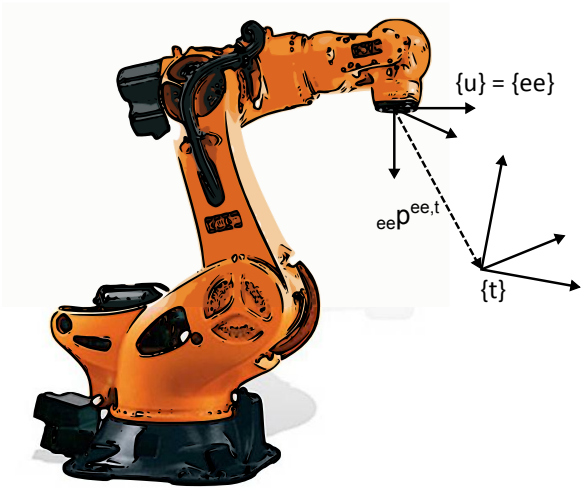


Fig. 1. Configuration of a robot holding a load.

natural representations [7]: *body-fixed*: $v = ee, f = ee$, *inertial*: $v = bs, f = bs$ and *hybrid*: $v = ee, f = bs$. Depending on the choice of the frames, the vectors ${}^{v}_{f}\boldsymbol{j}_{\boldsymbol{a}}{}^{o}_{w}$ and ${}^{v}_{f}\boldsymbol{j}_{\boldsymbol{b}}{}^{o}_{w}$ will be different, but the overall formulation of the optimization problem remains the same.

B. Inertial forces and torques acting on a load

If a robot is moving a load, indicated by load frame $\{t\}$ in figure 1 and attached to the robot at frame $\{u\}$, the acceleration of the robot will result in inertial forces and torques acting on that load. Figure 1 shows this set-up in the case of $\{u\} = \{ee\}$. In this section we show that these inertial forces and torques are linear in the optimization variables. Hence, constraints on these forces preserve convexity. In this paper we consider loads that do not move with respect to the frame $\{u\}$.

The load frame $\{t\}$ represents the frame with the principal axes of inertia of the load and has the center of gravity as its origin. Here ${}^{t}_{t}I$ is the inertia tensor for the principal axes and m the mass of the load. We assume that the load frame $\{t\}$ is translated with vector ${}_{u}\boldsymbol{p}^{u,t}$ ($\boldsymbol{p}$ as shorthand notation) and rotated with the constant rotation matrix ${}^{t}_{u}R$ with respect to the robot frame $\{u\}$ [8]. Since the load does not move with respect to $\{u\}$, $\boldsymbol{p}$ and ${}^{t}_{u}R$ are constants with respect to time t and the path coordinate s. Furthermore we have that ${}^{t}_{u}R = {}^{u}_{t}R^{T}$. The forces and torques acting on the load, due to the movement of the robot, are derived using the above description of the system.

1) Inertial force: The inertial force can be determined from general expressions of inertial forces in a frame moving with acceleration ${}^{u}_{u}\dot{\boldsymbol{t}}^{u}_{bs} = \left({}^{u}_{u}\dot{\boldsymbol{v}}^{u\,T}_{bs},\ {}^{u}_{u}\dot{\boldsymbol{\omega}}^{u\,T}_{bs}\right)^{T}$. The Coriolis terms are zero since the load does not move inside the robot frame $\{u\}$. The inertial force acting on the load $\{t\}$, attached to the robot at frame $\{u\}$, expressed in the load frame $\{t\}$, can be written as

$${}_{t}\boldsymbol{f}^{t[u]}_{(\text{iner})} = -m\ {}^{u}_{t}R\ [{}^{u}_{u}\dot{\boldsymbol{v}}^{u}_{bs} + {}^{u}_{u}\dot{\boldsymbol{\omega}}^{u}_{bs} \times \boldsymbol{p} + {}^{u}_{u}\boldsymbol{\omega}^{u}_{bs} \times ({}^{u}_{u}\boldsymbol{\omega}^{u}_{bs} \times \boldsymbol{p})]$$

Now using (9) and ${}^{u}_{u}\boldsymbol{t}^{u}_{bs} = \left({}^{u}_{u}\boldsymbol{v}^{u\,T}_{bs},\ {}^{u}_{u}\boldsymbol{\omega}^{u\,T}_{bs}\right)^{T} = {}^{u}_{u}\boldsymbol{j}_{\boldsymbol{a}}{}^{u}_{bs}\sqrt{b}$ (see (6)), the inertial force acting on the load, expressed in the load frame $\{t\}$, can be written as

$${}_{t}\boldsymbol{f}^{t[u]}_{(\text{iner})}(m, \boldsymbol{p}, s) = {}_{t}\boldsymbol{f}^{t[u]}_{\boldsymbol{a}}(m, \boldsymbol{p}, s)a(s) + {}_{t}\boldsymbol{f}^{t[u]}_{\boldsymbol{b}}(m, \boldsymbol{p}, s)b(s),$$

where

$${}_{t}\boldsymbol{f}^{t[u]}_{\boldsymbol{a}}(m, \boldsymbol{p}, s) = -m\ {}^{u}_{t}R\ [{}^{u}_{u}\boldsymbol{j}_{\boldsymbol{a_t}}{}^{u}_{bs}(s) + {}^{u}_{u}\boldsymbol{j}_{\boldsymbol{a_r}}{}^{u}_{bs}(s) \times \boldsymbol{p}],$$

$$\begin{aligned}{}_{t}\boldsymbol{f}^{t[u]}_{\boldsymbol{b}}(m, \boldsymbol{p}, s) = -m\ {}^{u}_{t}R\ [&{}^{u}_{u}\boldsymbol{j}_{\boldsymbol{b_t}}{}^{u}_{bs}(s) + {}^{u}_{u}\boldsymbol{j}_{\boldsymbol{b_r}}{}^{u}_{bs}(s) \times \boldsymbol{p} \\ &+ {}^{u}_{u}\boldsymbol{j}_{\boldsymbol{a_r}}{}^{u}_{bs}(s) \times ({}^{u}_{u}\boldsymbol{j}_{\boldsymbol{a_r}}{}^{u}_{bs}(s) \times \boldsymbol{p})],\end{aligned}$$

and $\boldsymbol{j}_{\boldsymbol{a_t}} = \begin{pmatrix}\mathbb{I}_3, & \boldsymbol{0}_{3\times3}\end{pmatrix}\boldsymbol{j}_{\boldsymbol{a}}$ (with identity matrix $\mathbb{I}_n \in \mathbb{R}^{n\times n}$), $\boldsymbol{j}_{\boldsymbol{a_r}} = \begin{pmatrix}\boldsymbol{0}_{3\times3}, & \mathbb{I}_3\end{pmatrix}\boldsymbol{j}_{\boldsymbol{a}}$, $\boldsymbol{j}_{\boldsymbol{b_t}} = \begin{pmatrix}\mathbb{I}_3, & \boldsymbol{0}_{3\times3}\end{pmatrix}\boldsymbol{j}_{\boldsymbol{b}}$ and $\boldsymbol{j}_{\boldsymbol{b_r}} = \begin{pmatrix}\boldsymbol{0}_{3\times3}, & \mathbb{I}_3\end{pmatrix}\boldsymbol{j}_{\boldsymbol{b}}$. Hence the constants in ${}_{t}\boldsymbol{f}^{t[u]}_{(\text{iner})}$ only depend on ${}^{u}_{t}R$, the mass m of the load, the position of the load $\boldsymbol{p}$, and the vectors $\boldsymbol{j}_{\boldsymbol{a}}$ and $\boldsymbol{j}_{\boldsymbol{b}}$.

2) Gravitational force: Gravity acting on the load, expressed in the load frame $\{t\}$, can be written as

$${}_{t}\boldsymbol{g}^{t[u]}(m, s) = {}^{u}_{t}R\ {}^{bs}_{u}R(s)\ (0, 0, -mg)^{T},$$

where ${}^{bs}_{u}R$ is the rotation matrix of the robot base frame $\{bs\}$ with respect to the robot frame $\{u\}$ and g is the gravitational acceleration.

3) Inertial torque: The inertial torque is the torque required to ensure the rotational motion of the load and can be described as

$${}_{t}\boldsymbol{\tau}^{t[u]}_{(\text{iner})} = -\left({}^{t}_{t}I\ {}^{u}_{t}R\ {}^{u}_{u}\dot{\boldsymbol{\omega}}^{u}_{bs} + ({}^{u}_{t}R\ {}^{u}_{u}\boldsymbol{\omega}^{u}_{bs}) \times \left({}^{t}_{t}I\ {}^{u}_{t}R\ {}^{u}_{u}\boldsymbol{\omega}^{u}_{bs}\right)\right),$$

which can be written as

$${}_{t}\boldsymbol{\tau}^{t[u]}_{(\text{iner})}({}^{t}_{t}I, s) = {}_{t}\boldsymbol{\tau}^{t[u]}_{\boldsymbol{a}}({}^{t}_{t}I, s)a(s) + {}_{t}\boldsymbol{\tau}^{t[u]}_{\boldsymbol{b}}({}^{t}_{t}I, s)b(s),$$

where

$${}_{t}\boldsymbol{\tau}^{t[u]}_{\boldsymbol{a}}({}^{t}_{t}I, s) = -{}^{u}_{t}R\ {}^{t}_{u}I\ {}^{u}_{u}\boldsymbol{j}_{\boldsymbol{a_r}}{}^{u}_{bs}(s),$$

$$\begin{aligned}{}_{t}\boldsymbol{\tau}^{t[u]}_{\boldsymbol{b}}({}^{t}_{t}I, s) = -{}^{u}_{t}R\ [&{}^{t}_{u}I\ {}^{u}_{u}\boldsymbol{j}_{\boldsymbol{b_r}}{}^{u}_{bs}(s) \\ &+ {}^{u}_{u}\boldsymbol{j}_{\boldsymbol{a_r}}{}^{u}_{bs}(s) \times ({}^{t}_{u}I\,{}^{u}_{u}\boldsymbol{j}_{\boldsymbol{a_r}}{}^{u}_{bs}(s))],\end{aligned}$$

where ${}^{t}_{u}I = {}^{t}_{u}R\,{}^{t}_{t}I\ {}^{t}_{u}R^{T}$. Hence the constants in ${}_{t}\boldsymbol{\tau}^{t[u]}_{(\text{iner})}$ only depend on ${}^{u}_{t}R$, the inertia tensor ${}^{t}_{t}I$ of the load and the vectors $\boldsymbol{j}_{\boldsymbol{a}}$ and $\boldsymbol{j}_{\boldsymbol{b}}$.

From here on we suppose the mass m, inertia I and position $\boldsymbol{p}$ of the load to be fixed, hence we neglect the dependency of the forces and torques upon these parameters for notational simplicity.

Forces and torques linear in the optimization variables

The forces (inertial and gravitational) and torques (inertial), acting on the load, are now stacked in the wrench

$$
\begin{aligned}
{}_t\boldsymbol{w}^{t[u]}(s) &= \begin{pmatrix} {}_t\boldsymbol{f}^{t[u]}(s) \\ {}_t\boldsymbol{\tau}^{t[u]}(s) \end{pmatrix} = \begin{pmatrix} {}_t\boldsymbol{f}^{t[u]}_{(\text{iner})}(s) + {}_t\boldsymbol{g}^{t[u]}(s) \\ {}_t\boldsymbol{\tau}^{t[u]}_{(\text{iner})}(s) \end{pmatrix}, \\
&= {}_t\boldsymbol{w}^{t[u]}_{\boldsymbol{a}}(s)a(s) + {}_t\boldsymbol{w}^{t[u]}_{\boldsymbol{b}}(s)b(s) + {}_t\boldsymbol{w}^{t[u]}_{\boldsymbol{c}}(s). \quad (10)
\end{aligned}
$$

with

$$
{}_t\boldsymbol{w}^{t[u]}_{\boldsymbol{a}}(s) = \begin{pmatrix} {}_t\boldsymbol{f}^{t[u]}_{\boldsymbol{a}}(s) \\ {}_t\boldsymbol{\tau}^{t[u]}_{\boldsymbol{a}}(s) \end{pmatrix}, \; {}_t\boldsymbol{w}^{t[u]}_{\boldsymbol{b}}(s) = \begin{pmatrix} {}_t\boldsymbol{f}^{t[u]}_{\boldsymbol{b}}(s) \\ {}_t\boldsymbol{\tau}^{t[u]}_{\boldsymbol{b}}(s) \end{pmatrix}
$$

$$
\text{and} \;\; {}_t\boldsymbol{w}^{t[u]}_{\boldsymbol{c}}(s) = \begin{pmatrix} {}_t\boldsymbol{g}^{t[u]}(s) \\ \boldsymbol{0} \end{pmatrix}.
$$

Hence, the wrench resulting from gravity and inertial forces and torques acting on a load, is linear in the optimization variables. This derivation is independent of the choice of $\{u\}$, which can be any frame on the robot.

IV. Applications

This section illustrates the convex framework for time-optimal path following with the proposed extensions given in Section III with five applications. First of all, a Cartesian acceleration twist constraint is added to the original optimization problem (5) in Section IV-A. A special case of this problem is the handling of fragile products, treated in Section IV-B. After this, the transportation of non-fixed bodies in the end effector frame is treated in 2D in Section IV-C and in 3D in Section IV-D. This results in inertial force and torque constraints.

The optimization problems considered in the applications are implemented in MATLAB using the free high-level optimization modeling tool YALMIP [9] on an Intel Core i3 CPU running at a 2.53GHz Windows machine. All numerical examples illustrating the applications are considering a seven degree of freedom robot executing a planar trajectory. The kinematic and dynamic parameters of the robot are given in the Appendix. The optimization problems are discretized as in [3].

A. Cartesian acceleration twist constraint

Here an example of a time-optimal motion with a Cartesian acceleration twist constraint is given (see III-A) by means of an experiment. In the experiment, a robot moves the end effector along a horizontal linear path, parallel to the y-axis of the robot base frame. Hence we consider only a body-fixed Cartesian acceleration of the end effector in the y-direction, which was limited to 5 m/s^2. In Fig. 2 the measured (full line) and the desired acceleration (dashed line) are plotted as a function of time.

It can be seen that the measured acceleration roughly follows the desired acceleration. However due to high, unmodelled, joint flexibilities there are large acceleration overshoots and vibrations. To enhance the performance these flexibilities should be incorporated in the dynamic model or jerk constraints could be added to constrain the excitation of the flexible resonant modes. However this would render the problem non-convex.

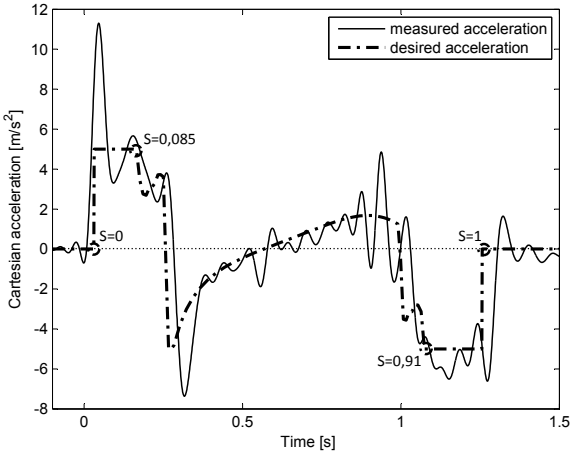


Fig. 2. Measured and desired y component of the body-fixed Cartesian acceleration twist of the end effector, constrained to 5 m/s^2.

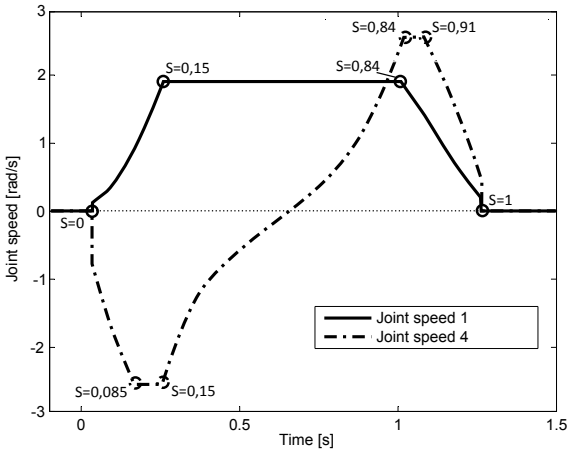


Fig. 3. Desired angular speed of joint one and four, constrained respectively to 1.9 rad/s and 2.5 rad/s.

For safety reasons, also the joint speed and joint acceleration was constrained in this experiment. Figure 3 shows the desired angular speed of joint 1 and 4. These two joint speed constraints and the Cartesian acceleration constraint are the only constraints that are determining (become active) in the optimization. We can see from these figures that the motion is of the bang-bang type since, at any s, one of these three constraints is active. This result was to be expected for a time-optimal motion.

B. Handling fragile products

If we want to handle fragile products with a robot, we must ensure that these products are not damaged. For a rigid body, the *damage boundary theorem* [5] states that the damage

boundary is a bound on the peak-acceleration acting on the body, also called the *fragility* $\mathcal{F}$. If the accelerations acting on the product exceed the bound, the product may be damaged. So when handling fragile products, one must ensure that the resulting acceleration (peak) on the body does not exceed the fragility, multiplied by a safety factor γ. This safety factor accounts e.g. for unmodelled flexibilities. It is relevant to take the fragility into account in the optimization problem since the fragility for items with delicate mechanical alignments (e.g. sensors, ...) goes down to $15g$ or less (where $1g = 9.81$ m/s^2) while accelerations of pick and place robots go up to $40g$ [10].

Suppose we have l products with mass m_i and frame $\{t_i\}$, attached to the robot at frame $\{u_i\}$ (e.g. the end effector frame $\{ee\}$). The origin of frame $\{t_i\}$ is the products center of gravity and lies at $\boldsymbol{p}_i$ with respect to the origin of the the robot frame $\{u_i\}$. Then, for the i-th ($i = 1, \ldots, l$) product, the constraint on the resulting translational acceleration, acting on the product, expressed in the product frame, can be formulated as

$$\left\| m^{-1} \left({}_{t_i}\boldsymbol{f}_{(\text{iner})}^{t_i[u_i]}(m_i, \boldsymbol{p}_i, s) + {}_{t_i}\boldsymbol{g}^{t_i[u_i]}(m_i, s) \right) \right\|_2 \leq \gamma_i \, \mathcal{F}_i \quad \text{for } \; i = 1, \ldots, l$$

We now define the translational acceleration

$$\begin{aligned} {}_{t_i}\boldsymbol{\alpha}^{t_i[u_i]}(s) &= m^{-1} \left({}_{t_i}\boldsymbol{f}_{(\text{iner})}^{t_i[u_i]}(m_i, \boldsymbol{p}_i, s) + {}_{t_i}\boldsymbol{g}^{t_i[u_i]}(m_i, s) \right) \\ &= {}_{t_i}\boldsymbol{\alpha}_{\boldsymbol{a}}^{t_i[u_i]}(m_i, \boldsymbol{p}_i, s) a(s) \\ &\quad + {}_{t_i}\boldsymbol{\alpha}_{\boldsymbol{b}}^{t_i[u_i]}(m_i, \boldsymbol{p}_i, s) b(s) + {}_{t_i}\boldsymbol{\alpha}_{\boldsymbol{c}}^{t_i[u_i]}(m_i, s) \end{aligned} \quad (11)$$

for $i = 1, \ldots, l$ where ${}_{t_i}\boldsymbol{\alpha}^{t_i[u_i]}(s) = (\boldsymbol{\alpha}_x, \boldsymbol{\alpha}_y, \boldsymbol{\alpha}_z)^T$ and $\boldsymbol{\alpha}_x$ is the x-component of the acceleration ${}_{t_i}\boldsymbol{\alpha}^{t_i[u_i]}(s)$. Hence, the constraint on the translational acceleration can be written as

$$\begin{aligned} \Big\| {}_{t_i}\boldsymbol{\alpha}_{\boldsymbol{a}}^{t_i[u_i]}(m_i, \boldsymbol{p}_i, s) a(s) + {}_{t_i}\boldsymbol{\alpha}_{\boldsymbol{b}}^{t_i[u_i]}(m_i, \boldsymbol{p}_i, s) b(s) \\ + {}_{t_i}\boldsymbol{\alpha}_{\boldsymbol{c}}^{t_i[u_i]}(m_i, s) \Big\|_2 \leq \gamma_i \, \mathcal{F}_i \quad \text{for } \; i = 1, \ldots, l \end{aligned}$$

Since the 2-norm of a convex function is a convex function, these l constraints preserve the convexity of the optimization problem.

Figure 4 shows the simulated resulting translational acceleration acting on the product, attached to the end effector, for a seven dof robot executing a linear path in the xy-plane under 45° with respect to the x-axis, without rotation of the end effector. We can see that the resulting translational acceleration is less than or equal to the fragility ($\mathcal{F} = 5$ m/s^2) multiplied by a safety factor ($\gamma = 0.45$).

C. Moving non-fixed bodies: 2D case

Suppose a body with frame $\{t\}$ lies, not fixed, on a plate attached to the frame $\{u\}$, here assumed to be the end effector frame $\{ee\}$, and it is desired that this body is transported

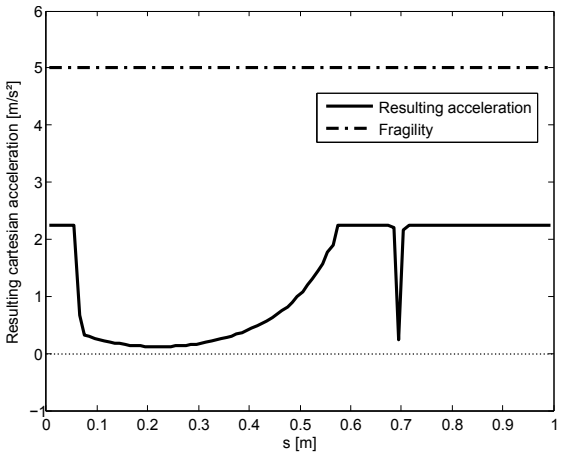


Fig. 4. Resulting translational acceleration constrained to be less than the fragility ($\mathcal{F} = 5$ m/s^2) multiplied by the safety factor ($\gamma = 0.45$).

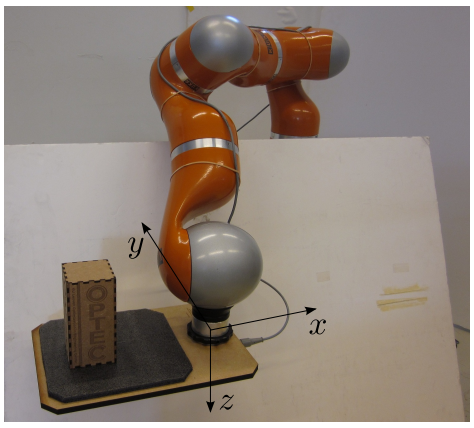


Fig. 5. Illustration of the proposed set-up for transporting non-fixed bodies.

time-optimally without moving on the plate or falling off. This requirement can be written as a set of convex constraints using the expression for the inertial forces and torques. Since the results of a 2D motion can be extrapolated to 3D motions, we first consider a rectangular body in a 2D motion along the $x-$axis in this section. The next section discusses the 3D case for a cylindrical and rectangular object.

We now assume that the plate lies in the end effector xy-plane and that the end effector z-axis is pointing downward when the plate is placed. The orientation of the plate with respect to the $\{ee\}$ frame remains constant during the motion. This set-up is shown in Figure 5. Suppose that forces ${}_t\boldsymbol{f}^{t[u]}(s) = (\boldsymbol{f}_x(s), \boldsymbol{f}_y(s), \boldsymbol{f}_z(s))^T$ and torques ${}_t\boldsymbol{\tau}^{t[u]}(s) = (\boldsymbol{\tau}_x(s), \boldsymbol{\tau}_y(s), \boldsymbol{\tau}_z(s))^T$ are acting on a rectangular object lying on a plate, where x, y and z denote the x, y and z component in the $\{t\}$ frame. Furthermore, it is supposed that there is Coulomb friction between the plate and the object with friction coefficient μ. Since the object is not fixed to the plate, three cases can be identified where the object starts to move. The object either starts to slip on the plate, tips over or lifts from

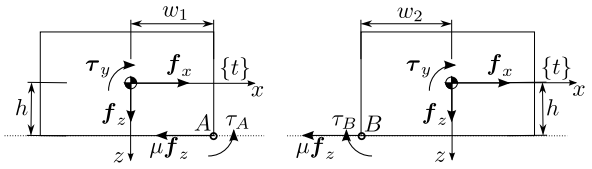


Fig. 6. Forces and torques acting on a rectangle just before tip around A (left) or B (right).

the plate.

From figure 6 it can be seen that there will be no slip if the resulting x-force $\boldsymbol{f}_x$ is smaller than the Coulomb friction force $f_c = \mu \boldsymbol{f}_z$. There will be no tip if the resulting inertial torque $\boldsymbol{\tau}_y + h\boldsymbol{f}_x$ around the corner A or $-(\boldsymbol{\tau}_y + h\boldsymbol{f}_x)$ around the corner B is smaller than the gravitation torque $w_1 \boldsymbol{f}_z$ or $w_2 \boldsymbol{f}_z$ respectively. This can be summarized as: no tip over corner A if the resulting torque $\tau_A = \boldsymbol{\tau}_y + h\boldsymbol{f}_x - w_1 \boldsymbol{f}_z$ at corner A is smaller than zero, and analogous for corner B if $\tau_B = -(\boldsymbol{\tau}_y + h\boldsymbol{f}_x) - w_2 \boldsymbol{f}_z$ is smaller than zero. There will be no lift if the resulting z-force $\boldsymbol{f}_z$ is bigger than zero. By defining the matrices

$$A_{2D} = \begin{pmatrix} 1 & 0 & 0 & 0 & 0 & 0 \end{pmatrix}, D_{2D} = \begin{pmatrix} 0 & 0 & 1 & 0 & 0 & 0 \end{pmatrix},$$

$$B_{2D} = \begin{pmatrix} h & 0 & 0 & 0 & 1 & 0 \\ -h & 0 & 0 & 0 & -1 & 0 \end{pmatrix}, C_{2D} = \begin{pmatrix} w_1 \\ w_2 \end{pmatrix}.$$

the constraints on the forces and torques can be summarized as constraints on the wrench ${}_t\boldsymbol{w}^{t[u]}$

$$\begin{aligned} \text{no slip:} \quad & |A_{2D}\ {}_t\boldsymbol{w}^{t[u]}| - \mu D_{2D}\ {}_t\boldsymbol{w}^{t[u]} < 0, \\ \text{no tipping over:} \quad & B_{2D}\ {}_t\boldsymbol{w}^{t[u]} - C_{2D} D_{2D}\ {}_t\boldsymbol{w}^{t[u]} < 0, \\ \text{no lift:} \quad & -D_{2D}\ {}_t\boldsymbol{w}^{t[u]} < 0, \end{aligned}$$

which are convex in ${}_t\boldsymbol{w}^{t[u]}$. The resulting optimization problem is then formulated as

$$\begin{aligned} \underset{a(.),b(.)}{\text{minimize}} \quad & \int_0^1 \frac{1}{\sqrt{b(s)}} ds, \\ \text{subject to} \quad & \boldsymbol{\tau}(s) = \boldsymbol{m}(s)a(s) + \boldsymbol{c}(s)b(s) + \boldsymbol{g}(s), \\ & \underline{\boldsymbol{\tau}}(s) \leq \boldsymbol{\tau}(s) \leq \overline{\boldsymbol{\tau}}(s), \\ & b(0) = \dot{s}_0^2, b(1) = \dot{s}_T^2, b(s) > 0, \\ & b'(s) = 2a(s), \\ & {}_t\boldsymbol{w}^{t[u]}(s) = {}_t\boldsymbol{w}_{\boldsymbol{a}}^{t[u]}(s)a(s) + {}_t\boldsymbol{w}_{\boldsymbol{b}}^{t[u]}(s)b(s) \\ & \quad + {}_t\boldsymbol{w}_{\boldsymbol{c}}^{t[u]}(s) \\ & |A_{2D}\ {}_t\boldsymbol{w}^{t[u]}(s)| - \mu D_{2D}\ {}_t\boldsymbol{w}^{t[u]}(s) < 0 \\ & B_{2D}\ {}_t\boldsymbol{w}^{t[u]}(s) - C_{2D} D_{2D}\ {}_t\boldsymbol{w}^{t[u]}(s) < 0 \\ & \quad - D_{2D}\ {}_t\boldsymbol{w}^{t[u]}(s) < 0 \\ & \text{for } s \in [0, 1]. \end{aligned}$$

Here, the mass and inertia of the plate and object are included in the robot model vectors $\boldsymbol{m}$, $\boldsymbol{c}$ and $\boldsymbol{g}$ as in [4].

D. Moving non-fixed bodies: 3D case

This section extends the reasoning for the 2D case to 3D cases. Again, the resulting constraints preserve the convexity of the optimization problem. Only two geometries are discussed (a rectangular prism and a cylinder) to keep the discussion brief, however, the same reasoning could be used for other geometries.

1) Rectangular Prism: Consider a rectangular prism standing on a plate attached to the robot. The ideas for the 2D rectangle are used here to derive constraints to prevent tipping over, slip and lift for the 3D prism. The definition of the dimensions of the body is analogous to the 2D case, where the width of the prism in the x or y direction is indicated with an index x or y.

There will be no translational slip if the resulting xy-force $f_r = || \left(\boldsymbol{f}_x, \boldsymbol{f}_y\right)^T ||_2$ is smaller than the Coulomb friction force $f_c = \mu \boldsymbol{f}_z$ (rotational slip is not considered here, but adding it would not affect convexity). To derive the tipping over constraints, we decouple the 3D prism as two 2D rectangles either in the x or y direction, since it can be shown that the object will always tip over one of the sides and not over the corner (only in an exceptional case where tipping over the corner is equivalent with tipping over the sides). We consider four possible tip situations: no tip over at edge A or B in the x-direction if $\tau_{A,x} < 0$ or $\tau_{B,x} < 0$ or in the y-direction if $\tau_{A,y} < 0$ or $\tau_{B,y} < 0$. To prevent lift, the downwards force $\boldsymbol{f}_z$ should again be bigger than zero.

By defining the matrices

$$A_{pr} = \begin{pmatrix} 1 & 0 & 0 & 0 & 0 & 0 \\ 0 & 1 & 0 & 0 & 0 & 0 \end{pmatrix}, D_{pr} = \begin{pmatrix} 0 & 0 & 1 & 0 & 0 & 0 \end{pmatrix},$$

$$B_{pr} = \begin{pmatrix} h & 0 & 0 & 0 & 1 & 0 \\ -h & 0 & 0 & 0 & -1 & 0 \\ 0 & h & 0 & 1 & 0 & 0 \\ 0 & -h & 0 & -1 & 0 & 0 \end{pmatrix}, C_{pr} = \begin{pmatrix} w_{x1} \\ w_{x2} \\ w_{y1} \\ w_{y2} \end{pmatrix}.$$

the constraints on the forces and torques can be summarized as constraints on the wrench ${}_t\boldsymbol{w}^{t[u]}$

$$\begin{aligned} \text{no slip:} \quad & ||A_{pr}\ {}_t\boldsymbol{w}^{t[u]}||_2 - \mu D_{pr}\ {}_t\boldsymbol{w}^{t[u]} < 0, \\ \text{no tipping over:} \quad & B_{pr}\ {}_t\boldsymbol{w}^{t[u]} - C_{pr} D_{pr}\ {}_t\boldsymbol{w}^{t[u]} < 0, \\ \text{no lift:} \quad & -D_{pr}\ {}_t\boldsymbol{w}^{t[u]} < 0, \end{aligned}$$

which are convex in ${}_t\boldsymbol{w}^{t[u]}$.

Figure 7 and 8 illustrate the results of an optimization for a seven dof robot, transporting a rectangular box with mass $m = 1$kg, moving along a circular trajectory in the $xy-$plane with radius 0.2m. The end effector, and hence the box, does not rotate during the trajectory and the x and y-axes of $\{ee\}$ and $\{t\}$ are aligned with the world frame x and y-axes. The set-up is shown in Figure 5. The box dimensions ($w_{x,1} = w_{x,2} = w_{y,1} = w_{y,2} = 0.025$ m and $h = 0.05$ m) and the friction between the plate and the box ($\mu = 0.8$) are chosen such that the tip constraint is dominant over the slip constraint.

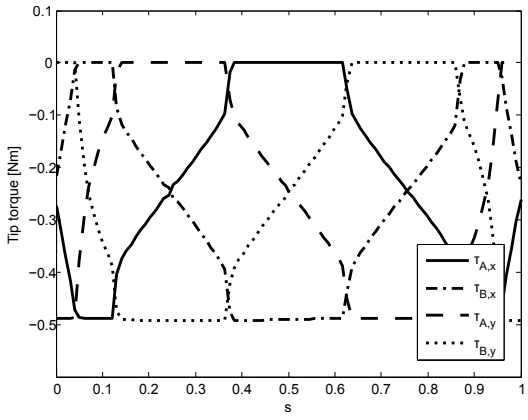


Fig. 7. Tipping torques as a function of s, acting on a rectangular prism

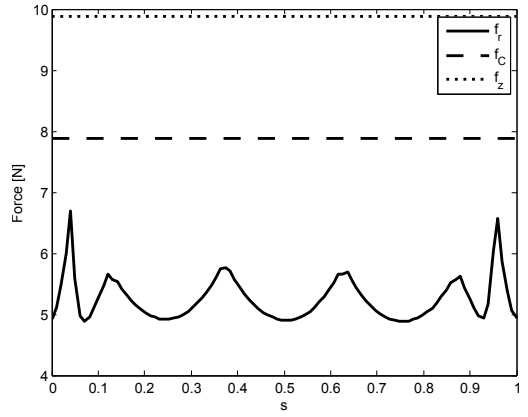


Fig. 8. Slip and lift forces as a function of s, acting on a rectangular prism

Figure 7 shows the tipping torques ($\tau_{A,x}, \tau_{B,x}, \tau_{A,y}$ and $\tau_{B,y}$), which are constrained to be less than zero, as a function of s. As can be seen from this figure, due to the time-optimal behaviour, there is always one active constraint. Depending on the $x+, x-, y+$ or $y-$ direction the robot is moving in, the respective tipping constraint will become active. Figure 8 shows that, due to the choice of the box dimensions, the slip constraint never becomes active, since the resulting xy-force f_r is always lower than the Coulomb friction force f_c. This figure also shows that, due to the horizontal trajectory, the lift constraint never becomes active since the downwards force is always bigger than zero (here equal to the constant gm where g is the gravitational acceleration).

2) Cylinder: Consider a cylinder standing on a plate attached to the robot. From figure 9 it can be seen that there will be no translational slip if the resulting xy-force $|| \left(\boldsymbol{f}_x, \boldsymbol{f}_y\right)^T ||_2$ is smaller than the Coulomb friction force $f_c = \mu \boldsymbol{f}_z$ (rotational slip is not considered here, but adding it would not affect convexity). There will be no tipping over if the resulting inertial xy torque $|| \left(\boldsymbol{\tau}_y + h\boldsymbol{f}_x, \boldsymbol{\tau}_x + h\boldsymbol{f}_y\right)^T ||_2$ around the bottom edge is smaller than the gravitational xy torque $r\boldsymbol{f}_z$. There will be no lift if the resulting z-force $\boldsymbol{f}_z$ is bigger than zero.

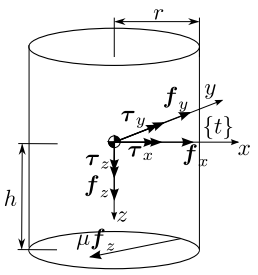


Fig. 9. Forces and torques acting on a Cylinder

By defining the matrices

$$A_{cy} = \begin{pmatrix} 1 & 0 & 0 & 0 & 0 & 0 \\ 0 & 1 & 0 & 0 & 0 & 0 \end{pmatrix}, B_{cy} = \begin{pmatrix} h & 0 & 0 & 0 & 1 & 0 \\ 0 & h & 0 & 1 & 0 & 0 \end{pmatrix},$$
$$D_{cy} = \begin{pmatrix} 0 & 0 & 1 & 0 & 0 & 0 \end{pmatrix}.$$

the constraints on the forces and torques can be summarized as constraints on the wrench ${}_t\boldsymbol{w}^{t[u]}$

$$\begin{aligned} \text{no slip:} \quad & ||A_{cy}\ {}_t\boldsymbol{w}^{t[u]}||_2 - \mu D_{cy}\ {}_t\boldsymbol{w}^{t[u]} < 0, \\ \text{no tipping over:} \quad & ||B_{cy}\ {}_t\boldsymbol{w}^{t[u]}||_2 - r D_{cy}\ {}_t\boldsymbol{w}^{t[u]} < 0, \\ \text{no lift:} \quad & -D_{cy}\ {}_t\boldsymbol{w}^{t[u]} < 0, \end{aligned}$$

These convex constraints are similar to the ones for the rectangular prism.

V. Conclusion

The Cartesian acceleration of the end effector of a robotic manipulator and the inertial forces and torques acting on a load can be written as a linear function of the optimization variables, for the convex path following problem (5) [3]. Using these results, a series of applications can be formulated that result in convex optimization problems. From the experiment in section IV-A we see that flexibilities in the joints of the robot result in oscillations on the desired Cartesian acceleration. In future work we will incorporate the effects of these flexibilities to enhance the performance.

Appendix

In this appendix we include the dynamic model of the considered robot. The kinematics of the robot are described using Denavit-Hartenberg coordinates [6]. Table I and II give the Denavit-Hartenberg coordinates and dynamic parameters, respectively, for each joint. Here I_{xx}, I_{yy} and I_{zz} represent the inertia [6] of each link, r_x, r_y and r_z represent the location of the center of gravity in the link frame [6] of each link. The mass m of each link is assumed to be 2 kg for each link.

Acknowledgment

This work benefits from K.U.Leuven-BOF PFV/10/002 Center-of-Excellence Optimization in Engineering (OPTEC), the Belgian Programme on Interuniversity Attraction Poles, initiated by the Belgian Federal Science Policy Office (DYSCO), the European research project EMBOCON FP7-ICT-2009-4 248940, project G.0377.09 of the Research Foundation –

link	α	a	θ	d
1	0	0	0	0.31
2	π/2	0	0	0
3	-π/2	0	0	0.4
4	-π/2	0	0	0
5	π/2	0	0	0.39
6	π/2	0	0	0
7	-π/2	0	0	0

TABLE I
DENAVIT-HARTENBERG COORDINATES FOR EACH JOINT.

link	(I_{xx}, I_{yy}, I_{zz}) [kg m^2]	(r_x, r_y, r_z) [m]	$\tau_{+,-}$ [Nm]
1	(0, 0, 0.0115)	(0, 0, 0)	$\pm$ 158
2	(-0.5472, 0, -0.54)	(0, -0.3, -0.0039)	$\pm$ 158
3	(0.0064, 0, 0.0108)	(0, -0.0016, 0)	$\pm$ 90
4	(-1.044, 0, -1.040)	(0, 0.5217, 0)	$\pm$ 90
5	(0.0037, 0, 0.006)	(0, 0.012, 0)	$\pm$ 90
6	(0.001, 0, 0.0036)	(0, 0.0081, 0)	$\pm$ 27
7	(0.001, 0, 0.12)$\cdot 10^{-3}$	(0, 0, 0)	$\pm$ 27

TABLE II
DYNAMIC PARAMETERS FOR EACH LINK

Flanders (FWO – Vlaanderen), and K.U.Leuven's Concerted Research Action GOA/10/11. Goele Pipeleers is a Postdoctoral Fellow of the Research Foundation - Flanders (FWO - Vlaanderen).

REFERENCES

[1] J. Bobrow, S. Dubowsky, and J. Gibson, "Time-optimal control of robotic manipulators along specified paths," *The International Journal of Robotics Research*, vol. 4, no. 3, pp. 3–17, 1985.

[2] K. Shin and N. Mckay, "Minimum-time control of robotic manipulators with geometric path constraints," *Automatic Control, IEEE Transactions on*, vol. 30, no. 6, pp. 531–541, 1985.

[3] D. Verscheure, B. Demeulenaere, J. Swevers, J. De Schutter, and M. Diehl, "Time-optimal path tracking for robots: A convex optimization approach," *Automatic Control, IEEE Transactions on*, vol. 54, pp. 2318 –2327, oct. 2009.

[4] F. Debrouwere, W. Van Loock, G. Pipeleers, M. Diehl, J. Swevers, and J. De Schutter, "Time-optimal robot path following with cartesian acceleration constraints: a convex optimization approach," in *Mechatronics Forum, LINZ, Austria*, pp. 469–475, 2012.

[5] R. E. Newton, "Fragility assessment theory and test procedure," Monterey Research Labs, 1968.

[6] M. W. Spong, *Robot Dynamics and Control*. New York, NY, USA: John Wiley & Sons, Inc., 1st ed., 1989.

[7] H. Bruyninckx and J. D. Schutter, "Symbolic differentiation of the velocity mapping for a serial kinematic chain," *Mechanism and Machine Theory*, vol. 31, no. 2, pp. 135 – 148, 1996.

[8] J. J. Craig, *Introduction to Robotics: Mechanics and Control*. Boston, MA, USA: Addison-Wesley Longman Publishing Co., Inc., 2nd ed., 1989.

[9] J. Löfberg, "Yalmip : A toolbox for modeling and optimization in MATLAB," in *Proceedings of the CACSD Conference*, (Taipei, Taiwan), 2004.

[10] F. Pierrot, C. Baradat, V. Nabat, O. Company, S. Krut, and M. Gouttefarde, "Above 40g acceleration for pick-and-place with a new 2-dof pkm," in *Robotics and Automation, 2009. ICRA '09. IEEE International Conference on*, pp. 1794 –1800, may 2009.